

The Disruption of Stellar Clusters Containing Massive Black Holes near the Galactic Center

M. Atakan Gürkan and Frederic A. Rasio

*Department of Physics and Astronomy, Northwestern University, Evanston, IL 60208
ato, rasio@northwestern.edu*

ABSTRACT

We present results from dynamical Monte Carlo simulations of dense star clusters near the Galactic center. These clusters sink toward the center of the Galaxy by dynamical friction. During their inspiral, they may undergo core collapse and form an intermediate-mass black hole through runaway collisions. Such a cluster can then reach within a parsec of the Galactic center before it completely disrupts, releasing many young stars in this region. This scenario provides a natural explanation for the presence of the young stars observed near the Galactic center. Here we determine the initial conditions for this scenario to work and we derive the mass distribution of cluster stars as a function of distance from the Galactic center. For reasonable initial conditions, we find that clusters massive enough for rapid inspiral would include more massive stars ($m_* \gtrsim 30 M_\odot$) than currently observed in the inspiral region. We point out several possible explanations for this apparent discrepancy.

Subject headings: black hole physics — Galaxy: center — galaxies: star clusters — methods: N-Body simulations, stellar dynamics

1. Introduction

Multi-wavelength observations of the Galactic center (GC) have revealed a supermassive black hole (SBH) and a stellar cusp surrounding it. The mass of the SBH, $M_{\text{SBH}} \simeq 4 \times 10^6 M_\odot$, is one of the most reliable estimates for massive black holes at the centers of galaxies. The stellar population within 1 pc of the SBH contains a variety of young and massive stars. Some of them are only about 20 Myr old and get as close as a few light days to the SBH; while from 0.1 to 0.4 pc even younger stars are found with ages 3 to 7 Myr. The presence of these young stars in the immediate vicinity of the SBH poses a problem known as the *youth paradox*. Their *in situ* formation is problematic since the SBH has a strong tidal influence

in this region. However, the time required for the migration of these stars from > 1 pc by dynamical friction would exceed their inferred ages, unless the migration rate is somehow accelerated.

In addition to their youth, these stars exhibit some peculiar dynamical properties. One of them is strong clustering. The sources IRS 16 and IRS 13 were initially thought to be single sources but later resolved into multiple components. IRS 16 is a collection of young (3–7 Myr) He I emission-line stars lying $1''$ – $7''$ in projection from Sgr A*. They form a co-moving group that is counter-rotating with respect to the Galaxy. IRS 13 is another complex, composed of hot bright stars, about $3.6''$ south-west of Sgr A*. In particular, IRS 13E is a compact, massive star cluster which is a few million years old (Maillard et al. 2004). Genzel et al. (2003) and Horrobin et al. (2004) find that the young He I emission-line stars in the vicinity of Sgr A* are all concentrated in two disks, forming two co-moving (but not gravitationally bound) populations. In addition to the clustering, stars within ~ 0.04 pc of Sgr A*, which are about 10 Myr old, seem to have higher than normal eccentricities (Schödel et al. 2003), but this anomaly may be explained by selection effects (Ghez et al. 2004).

One possible explanation for the presence of these young stars is that they are not young but *rejuvenated*. A possible path to rejuvenation, stellar mergers, is shown not to be viable by Genzel et al. (2003). Another path, squeezars, heating of stars by close tidal encounters with the SBH also fails to explain the observed population (Alexander & Morris 2003).

Aside from rejuvenation, another possible scenario, especially suggested by the observations of the two counter rotating and coeval disks of young stars around the SBH, is the infall and collision of two molecular clouds in the vicinity of the SBH. Such a collision may provide the required densities for star formation. Genzel et al. (2003) suggest that the stars resulting from the two colliding clouds will form two co-moving populations. However, since a collision leading to high densities will be highly inelastic, it is not clear that two distinct populations will form. To our knowledge, the collision and further evolution of dense clouds in the vicinity of a SBH has never been studied in detail. So, it is hard to decide whether this is a viable scenario.

A possibility that we investigate in this paper is the inspiral of a star cluster by dynamical friction, as suggested by Gerhard (2001). Portegies Zwart et al. (2003) carried out N -body simulations to study this scenario. The clusters in their simulations disrupted at > 1 pc from the GC, so cannot explain the presence the young star population very close to Sgr A*. Kim & Morris (2003), again using N -body simulations, concluded that, for a cluster to reach within the central parsec, it must either be very massive ($> 10^6 M_\odot$) or have formed near the GC (at < 5 pc). They found that, in both cases, a very high central density ($\sim 10^8 M_\odot \text{pc}^{-3}$) is required, and concluded that this scenario is implausible.

Hansen & Milosavljević (2003) suggested that the presence of an intermediate-mass black hole (IMBH) can stabilize a cluster so that survival all the way to within the central parsec can be achieved with much lower central densities. In addition, they suggested that an IMBH–SBH binary can perturb the young stars into radial orbits with small semi-major axes in a way similar to the Jupiter–Sun system creating short period comets (Quinn et al. 1990).

Kim et al. (2004) performed N -body simulations similar to those of Kim & Morris (2003) but with an additional IMBH embedded in the inspiraling cluster. They found that an IMBH does decrease the requirement for a high central density, but its mass must be about 10% of the total cluster mass. Since this is much larger than estimates of the collapsed core mass in dynamical simulations (0.1-0.2%; see Portegies Zwart & McMillan 2002; Gürkan et al. 2004) they concluded that a realistic IMBH cannot help transport young stars into the central parsec. However, after core collapse, the central object can continue to grow by colliding with the stars that migrate to the center by relaxation. This growth continues until the massive stars start evolving off the main sequence and lead to cluster expansion by mass loss through winds and supernovae (Portegies Zwart et al. 2004; Freitag et al. 2004).

Using our dynamical Monte Carlo code, we have carried out simulations where we form an IMBH through runaway collisions following core collapse during the cluster’s inspiral towards the GC. We discussed some initial results in a previous paper (Gürkan & Rasio 2004). Here we present all our results from simulations of dense star clusters near the GC using a more realistic Galactic mass distribution. We investigate the initial conditions required for these clusters to reach the GC within 3–10 Myr *and* undergo core collapse before disruption. In §2 we describe our numerical technique for cluster simulations and the inspiral mechanism. We present some semi-analytic calculations in §3, and the results of our full simulations in §4. We discuss these results and present our conclusions in §5.

2. Initial Conditions and Numerical Technique

For our simulations, we use a Monte Carlo technique, which provides an ideal compromise in terms of speed and accuracy. It has the star-by-star nature of the N -body techniques but incorporates physical assumptions which lead to simplifications, reducing the computation time. As a result, we can carry out simulations of systems with $N \gtrsim 10^7$ stars in $\lesssim 100$ CPU hours. For details of our method, we refer to our previous work (see Joshi et al. 2000, 2001 and references therein for basics, and Gürkan et al. 2004 for treatment of the realistic mass functions). Here we only explain in detail the additions to our code for this paper.

2.1. Initial conditions and Units

For the initial mass function (IMF) we implemented a Salpeter distribution, $dN/dm \propto m^{-2.35}$, with $m_{\min} = 0.2 M_{\odot}$ and $m_{\max} = 120 M_{\odot}$. Other choices of IMF, e.g., Miller-Scalo or Kroupa, do not change the core collapse time, as long as $m_{\max}/m_{\min} \gtrsim 100$ (Gürkan et al. 2004).

For the initial structure of our clusters we chose King models (see Binney & Tremaine 1987, Chapter 4). This choice allows us to implement the initial tidal cutoff in a natural way. In addition, the rate of evolution of the system, which is determined by the central relaxation time (Gürkan et al. 2004), can be adjusted by a single parameter, the dimensionless central potential W_0 . For the sake of simplicity we chose the tidal radius of the King model equal to the Jacobi radius of the cluster. (see §2.3)

Throughout this paper we use standard Fokker-Planck units (Hénon 1971): $G = M_0 = -4E_0 = 1$, where G is Newton’s gravitational constant, M_0 is the initial total mass of the cluster, and E_0 is the initial total energy. The conversion to physical units is done by calculating the physical mass of the system, and identifying the tidal radius of the King model used with the Jacobi radius. Various length and time scales of King models are given in Table 1 of Gürkan et al. (2004).

2.2. Boundary Condition at the Center

In the continuum limit, when a cluster undergoes core collapse, the central density becomes infinite in a finite time. In addition to being unphysical, high densities require small timesteps and render the dynamical evolution of the system impossible to follow numerically. When various physical processes and the finite radii of stars are taken into account, the central density cannot increase indefinitely. This can result from energy generation by “three-body binaries” (Giersz 2001, and references therein), “burning” of primordial binaries (Fregeau et al. 2003, and references therein) or physical collisions. For the young dense clusters we consider here, we expect energy generation from binary formation or binary burning to play a minor role, since for these systems, an interaction with a hard binary is likely to lead to a merger (Fregeau et al. 2004).

The local collision time, i.e., the average time after which a star has experienced one collision, is given by

$$t_{\text{coll}} \simeq 2.1 \times 10^{12} \text{ yr} \frac{10^6 \text{ pc}^{-3}}{n} \frac{\sigma_v}{30 \text{ km s}^{-1}} \frac{R_{\odot}}{R_*} \frac{M_{\odot}}{M_*}, \quad (1)$$

where σ_v is the velocity dispersion, n is the number density of stars, R_* and M_* are the radius and the mass of the star under consideration. In the systems we consider in this paper, t_{coll} is larger than the lifetime of the cluster except for the stars participating in the core collapse. We used an approximation to exploit this property. Rather than treating collisions explicitly as in Freitag & Benz (2002), we introduced a simple boundary condition near the center of the cluster: when a star is part of the collapsing core, we add its mass to a growing central point mass and remove it from the simulation. This central point mass is then used only during the calculation of the cluster gravitational potential. We determine whether a star is part of the collapsing core by monitoring its orbit’s apocenter. We have chosen this criterion rather than one based on pericenter or instantaneous position to guarantee that the stars under consideration are restricted to a small region near the center. The threshold value we have chosen for the apocenter distance is 2×10^{-4} in Fokker-Planck units. For our models, t_{coll} within this radius is $\sim 10^4$ yr, i.e., all stars restricted to this region will rapidly undergo collisions. We determined the threshold value empirically. Choosing a large value leads to removal of stars from the system before core collapse. Choosing a very small value is also problematic because of the very short collision times. If collisions are not taken into account, a few massive stars sinking to the center of the cluster could easily reach energies comparable to the total energy of the cluster and have a substantial effect on the evolution of the system (Hénon 1975, and references therein). We found that threshold values in the range 5×10^{-5} – 3×10^{-4} generally avoid these problems and 2×10^{-4} is a number suitable for all the clusters we simulated.

We compared the rate of growth of the central mass in our simulations with results from other Monte Carlo simulations where collisions between the stars are treated more realistically Freitag et al. (2005,b). We found that we typically underestimate the rate of growth slightly, by 20 to 30%. We have also compared the evolution of the average mass among the innermost 5 000 stars and found that, in our simulations, the increase in average mass slightly lags behind, but reaches the same final value. This is probably related to the slower growth of the central mass in our code. It is not possible to determine which results are more accurate as these simulations cannot be repeated with more direct methods. In any case we do not expect this small difference to affect our results significantly.

2.3. Tidal Truncation

During the course of our simulations, we remove the stars that gain positive energies because of interactions, or whose apocenter lies beyond the cluster’s tidal radius. This tidal radius depends on the mass distribution in the GC region and the cluster’s current position.

The tidal radius of the cluster can be estimated by using the following expression for the Jacobi radius

$$r_J \simeq \left[\frac{m_J}{2M(R)} \right]^{1/3} R, \quad (2)$$

where m_J is the bound mass of the cluster, R is the distance from the GC, and $M(R)$ is the mass within a circular orbit at this radius. The latest estimate for the Galactic mass distribution near the central BH is given by Genzel et al. (2003). They estimate the *stellar* mass density as a broken power law,

$$\rho_\star(R) = 1.2 \times 10^6 \left(\frac{R}{R_b} \right)^{\alpha-3} M_\odot \text{ pc}^{-3}, \quad (3)$$

with $\alpha = 1.63$ for $R \leq R_b$, $\alpha = 1.0$ for $R > R_b$, and $R_b = 0.38$ pc. This mass distribution is a self-consistent description that goes all the way from 0.1 to about 10 pc, but much farther than that it may underestimate the stellar density (Tal Alexander, private communication). We derive the formulae for dynamical friction on a point mass, resulting from a broken power law mass density distribution and an additional central BH of mass $M_{\text{SBH}} = 4 \times 10^6 M_\odot$ (Melia & Falcke 2001; Ghez et al. 2003; Schödel et al. 2003), in Appendix A. As a result of the dynamical friction, the distance of the cluster from the GC changes continuously; we include the effect of this change by adjusting r_J appropriately in our simulations.

In principle, the treatment we use for dynamical friction is valid only for point masses and extended clusters require a modification of this treatment. However, the finite size affects only the Coulomb logarithm in equation A5, and, as long as the size of the cluster (r_h) is small with respect to the size of the region that contributes to the dynamical friction, this leads only to a small decrease in the drag on the cluster (Binney & Tremaine 1987, § 7.1). Since this condition is always satisfied in our simulations, we do not expect our results to be affected by this approximation. McMillan & Portegies Zwart (2003) established numerically the validity of the formulation we use by making comparisons to more exact N -body simulations.

3. Semi-analytical calculations

For a point mass, the time required to reach the GC from an initial distance R_0 can be calculated by integrating equations (A9) and (A11). Since equation (A9) has a logarithmic singularity near the origin, for the calculations below, we stop the integration at $R = 0.01$ pc. Most of the mass loss from the cluster takes place near the center, so neglecting the mass loss provides a reasonable first estimate for the inspiral time, t_{in} . Possible upper limits for t_{in} are 3 or 10 Myr, which are about the lifetimes of the brightest IR stars observed near the

GC. By requiring the cluster to undergo core collapse before reaching the GC, we can also obtain a lower limit for t_{in} . This can be transformed into a condition on the initial structure of the cluster using $t_{\text{cc}} \simeq 0.15 t_{\text{rc}}(0)$ (Gürkan et al. 2004), where $t_{\text{rc}}(0)$ is the initial central relaxation time. We illustrate these constraints in Figure 1. The solid lines correspond to the upper limits on t_{in} from the stellar evolution timescale. Above these lines it takes more than the denoted time (3 or 10 Myr) to reach 0.01 pc for a point mass. The bow-like dashed lines correspond to lower limits for various King models. To the right of these lines, the inspiral time for a point mass is shorter than the core collapse time, hence runaway collisions cannot happen unless the system is initially collisional. For these calculations we have computed the timescales for the King models by assuming their tidal radius is initially equal to their Jacobi radius given in Equation 2. In this figure we also show results of some of our simulations (see next section).

The next step in approximation is using a realistic structure for the cluster but neglecting the changes in structure during the inspiral. Since the structure changes on a relaxation timescale and in the outer parts of the cluster the relaxation time is much longer than the inspiral time, this approximation provides a good estimate for the mass loss during the inspiral, at least until close to disruption. We have computed the rate of inspiral of different King models for different initial distances from the GC and initial cluster masses. We present our results for initial distance $R_0 = 10$ pc in Figure 2. During the inspiral we calculate the change in bound mass as follows. First we calculate the tidal radius by using the current mass and distance from the GC by equation (2). From this and the structure of the given King model a new bound mass is calculated. This procedure is repeated until the bound mass converges to a value. Failure of convergence marks the disruption.

In Figures 2 and 3 we show the results of our calculations for extended clusters. Unlike a point-mass, an extended cluster disrupts at a finite distance from the GC, R_{dis} . This distance decreases as more of the cluster’s mass is concentrated near its center, but is independent of the total mass in the cluster. The inspiral time, on the other hand, has a strong dependence on the total mass. The independence of R_{dis} from total mass can be understood as follows. For a given W_0 , the disruption happens when the tidal radius reaches a specific fraction of the initial Jacobi radius. The relation between this value and the distance from the GC is independent of the initial cluster mass, since more massive clusters start with a proportionately larger initial Jacobi radius. This is also the main reason for the dependence of R_{dis} on initial distance. Note that, in principle, a cluster can underfill its Jacobi radius at formation, i.e., clusters formed at large distances can have the same size as the clusters formed close to the GC. The disruption radii we obtain in this approximation are upper limits since mass segregation, the formation of a cusp, and the subsequent IMBH will all increase the mass concentration towards the center.

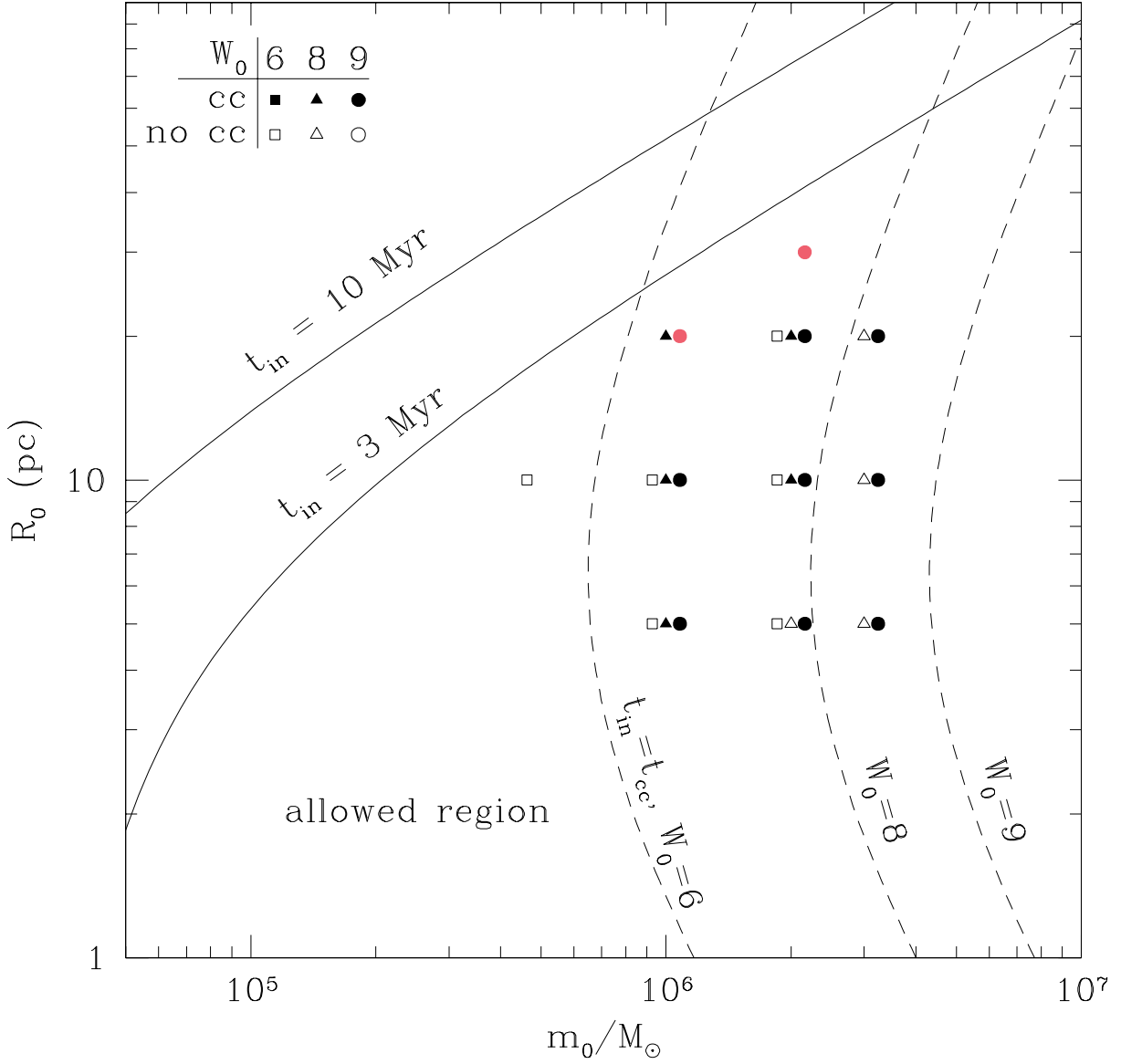


Fig. 1.— Region of R_0 - m_0 space that allows fast inspiral (denoted by solid lines) and core collapse happening during inspiral (for various King models; denoted by dashed lines), in the point-mass approximation. Results of various simulations are shown with symbols of different shapes, corresponding to different initial structure; full symbols are for systems that experienced core collapse and open symbols correspond to systems that disrupted before core collapse. All models shown have $t_{\text{dis}} < 3$ Myr except for the ones with gray symbols (colored red in the electronic edition), which have $3 \text{ Myr} < t_{\text{dis}} < 4 \text{ Myr}$

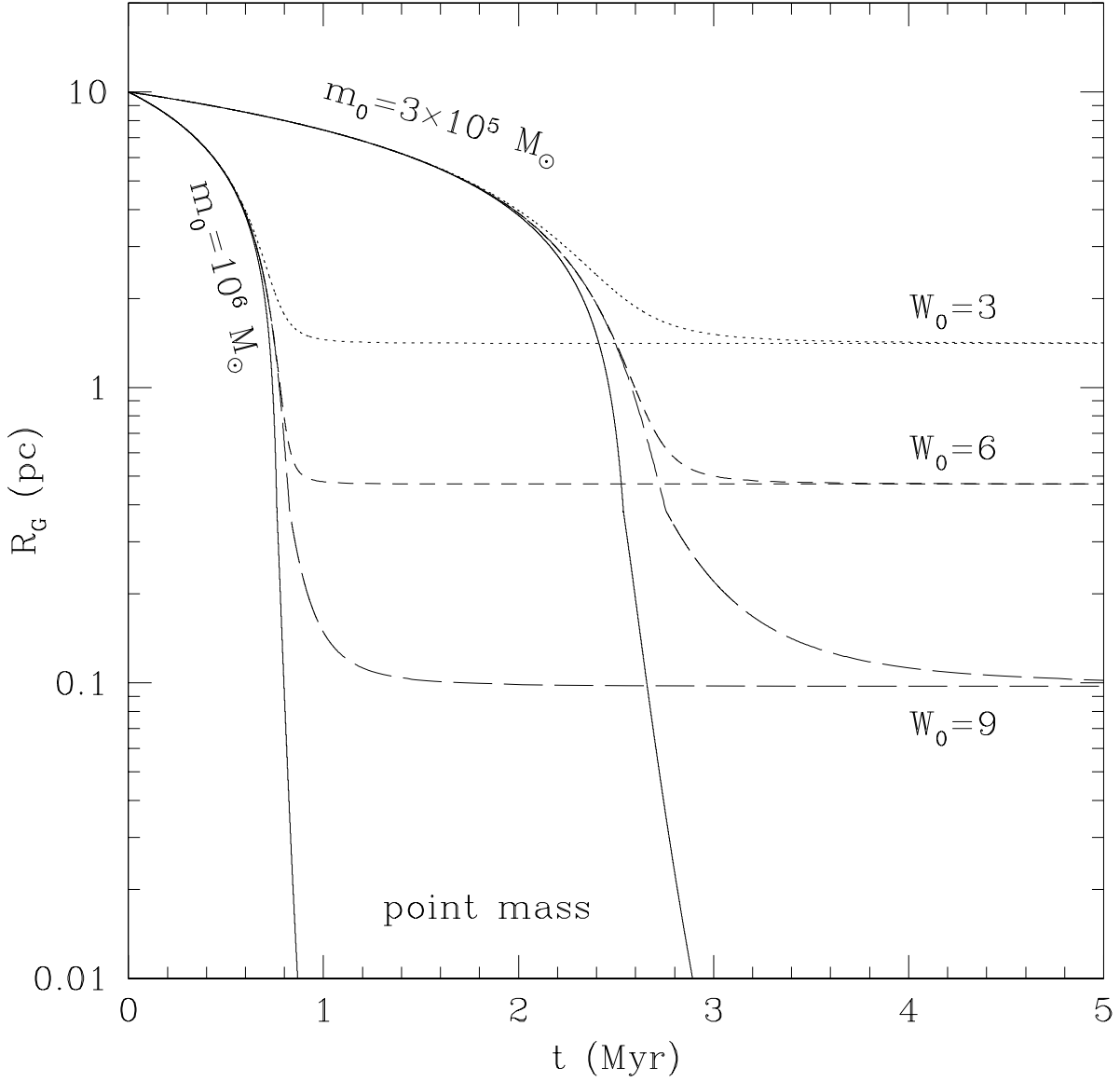


Fig. 2.— Rate of inspiral for point-mass and King models. The two families of curves correspond to initial masses $m_0 = 3 \times 10^5 M_\odot$ and $m_0 = 10^6 M_\odot$. For each initial mass, results are shown for point-mass (solid line) and King models with $W_0 = 9$ (long-dashed line), $W_0 = 6$ (dashed line), and $W_0 = 3$ (dotted line).

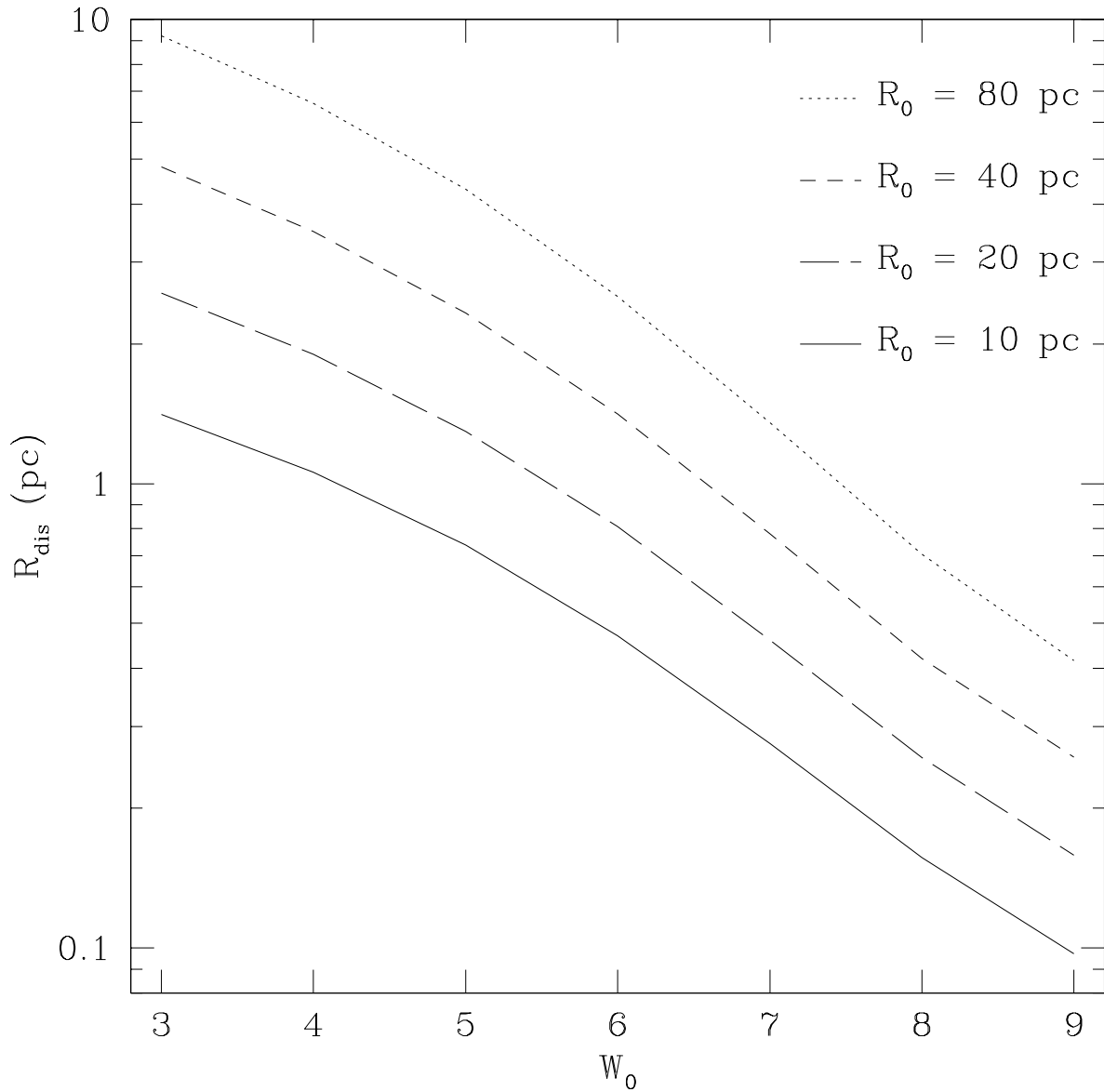


Fig. 3.— Dependence of disruption radius R_{dis} on initial concentration and initial distance.

These calculations show that for a wide region of $R_0 - m_0$ parameter space it is plausible that a cluster can reach to within a fraction of a parsec of the GC in a few million years. A high initial concentration ($W_0 \gtrsim 8$) is required for the cluster not to disrupt too far from the GC, as well as to guarantee rapid core collapse. More detailed simulations are required to verify and establish these findings, and to obtain the demographics of the stars that reach the GC. To illustrate this point, we present a comparison of point-mass and extended cluster models with a full simulation (Model5c, see next section) in Figure 4. All calculations presented in this figure start with the same initial mass and initial distance from the GC. This comparison shows that the effects of dynamical evolution, namely the enhanced mass loss due to expansion, can be quite important. Note that, for clusters with lower initial concentrations, the relaxation will be slower and the difference between full simulation and the extended static model will be smaller. However the deviations from the point-mass approximation will be larger.

4. Results of simulations

4.1. Overview of results

We have performed simulations starting with King models of dimensionless central potentials $W_0 = 6, 8$, and 9 at a variety of distances and initial masses. We present our results in Table 1. We ended our simulations when the number of stars in the cluster dropped to 0.5% of its initial value. We defined this as the point of disruption and denoted the time to reach this point and distance from GC with t_{dis} and R_{dis} , respectively. Allowing the cluster to evolve beyond this point will not change our results since, at this point, the mass is so low that dynamical friction is no longer effective, and the distance from the GC remains constant. In addition, as a result of the low number of stars, relaxation and the consequent evaporation of the cluster will be very rapid. Most of the clusters with high initial concentration went into core collapse before disruption and the central point mass described in §2 grew during the inspiral. This accumulated mass is indicated in column 7 of our table. For less dense clusters, the inspiral is faster than the core collapse and in those cases no central point mass is grown. We did not observe significant post-core-collapse expansion in our simulations. The growth of the central mass indicates that segregation of massive stars continue beyond the core collapse.

An overview of the results shows that neglecting the changes in the structure of the cluster during its inspiral provides a good estimate for the time to disruption, t_{dis} . However, this is not true for R_{dis} , which is dependent on the total initial mass for an evolving cluster. This dependence is a result of the interplay between inspiral time and relaxation time. For

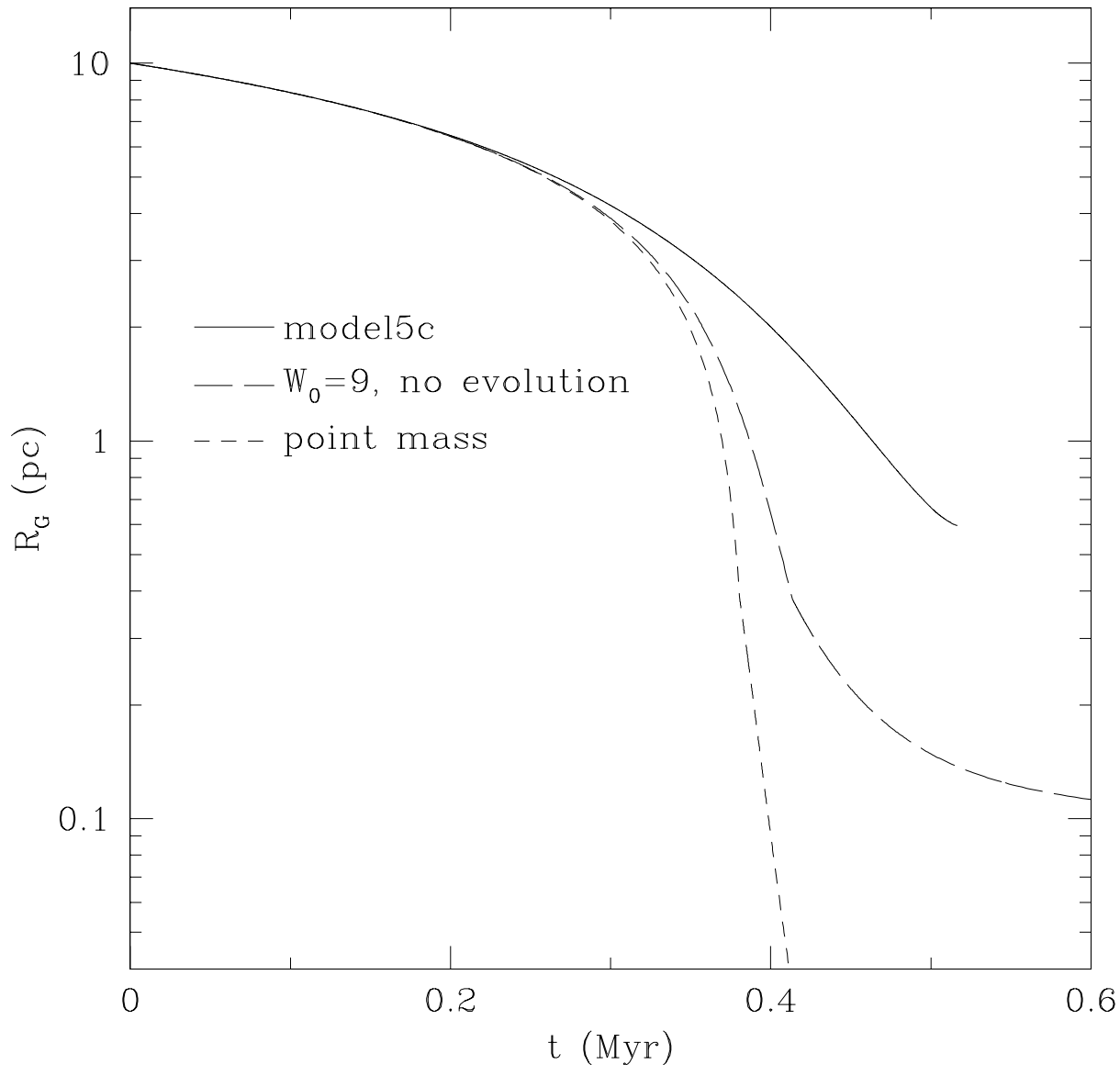


Fig. 4.— Comparison of a full simulation with an extended static model and the point-mass approximation.

Table 1. Results of Simulations

model ID	m_0 (M_\odot)	R_0 (pc)	W_0	R_{dis} (pc)	t_{dis} (Myr)	m_{cen} (M_\odot)
1a.....	3×10^6	20	8	1.04	1.04	-
2a.....	3×10^6	10	8	0.35	0.31	-
3a.....	3×10^6	5	8	0.22	0.12	-
4a.....	2×10^6	20	8	1.58	1.59	3000
5a.....	2×10^6	10	8	0.88	0.46	580
6a.....	2×10^6	5	8	0.34	0.17	-
7a.....	10^6	20	8	1.89	3.16	3600
8a.....	10^6	10	8	0.98	0.94	2500
9a.....	10^6	5	8	0.47	0.32	2000
4b	2×10^6	20	6	1.44	3.00	-
5b	2×10^6	10	6	0.42	0.85	-
6b	2×10^6	5	6	0.24	0.31	-
7b	10^6	20	6	2.09	3.08	-
8b	10^6	10	6	0.92	0.88	-
9b	10^6	5	6	0.42	0.30	-
10b ...	5×10^5	20	6	4.59	2.96	560
11b ...	5×10^5	10	6	1.55	0.86	-
12b ...	3×10^5	20	6	4.44	3.00	1200
13b ...	3×10^5	10	6	2.31	0.80	-
1c.....	3×10^6	20	9	1.23	1.10	5500
2c.....	3×10^6	10	9	0.56	0.35	4500
3c.....	3×10^6	5	9	0.28	0.14	3000
4c.....	2×10^6	20	9	1.20	1.70	6000
5c.....	2×10^6	10	9	0.60	0.52	4900
6c.....	2×10^6	5	9	0.33	0.20	4200
7c.....	10^6	20	9	1.89	3.23	4700
8c.....	10^6	10	9	0.76	1.04	3500
9c.....	10^6	5	9	0.43	0.34	3600
10c....	5×10^5	20	9	3.14	6.50	2900
11c....	5×10^5	10	9	1.26	1.95	2700
12c....	3×10^5	20	9	4.18	11.0	1900
13c....	3×10^5	10	9	1.91	3.04	2000
17c....	2×10^6	30	9	1.96	3.54	6800
18c....	2×10^6	60	9	5.17	13.8	6800
19c....	2×10^6	50	9	3.81	9.63	6600

Note. — The first column is the model ID. The following three columns indicate the initial conditions of the cluster: mass in solar masses, initial distance from the GC in parsecs and the dimensionless central potential. The last three columns are the results of the simulations: the disruption distance in parsecs, the time it takes for disruption in Myr, and the accumulated mass at the center of the cluster in solar masses. If the cluster disrupts before going into core collapse, no mass is accumulated at the center. In these cases a hyphen is used in the last column.

a massive cluster containing a large number of stars, the inspiral time is short but the relaxation time is long. Hence only the central part of the cluster has time to evolve. For a less massive cluster the outer parts have time to evolve and expand. As a result, the mass loss is enhanced and the disruption happens at a further distance from the GC.

In Figure 1 we plot the results of some our simulations to compare with point-mass estimates. We have only plotted models where disruption distance from the GC was small. For models started with $R_0 \leq 10$ pc, only the ones within 1 pc of the GC; and for the others only the ones disrupted within 2 pc of GC are plotted. We have used black symbols for models with $t_{\text{dis}} < 3$ Myr, and gray symbols (colored red in the online version) otherwise. We find that inspiral and/or disruption time in simulations exceed the estimated inspiral time from point-mass approximation. Similarly, the disruption distance is always larger in full simulations than static cluster approximations. Finally, sometimes clusters disrupt without going into core collapse in simulations where the point-mass approximation predicts core collapse times shorter than inspiral times. These results show that semi-analytical approximations provide necessary but not sufficient conditions for our scenario to work. Increasing the realism by taking the tidal mass loss of the cluster and its expansion into account cannot be compensated by the increase in central density of the cluster, and leads to disruption happening earlier and/or further from the GC than indicated by the semi-analytical methods. It is not possible to resolve the core-collapse criterion, indicated by dashed lines in Figure 1, for $W_0 = 6, 9$ models as is done for $W_0 = 8$ case. For $W_0 = 6$, the boundary is at low initial mass which correspond to low number of stars. Such clusters have short relaxation times and hence expand and disrupt rapidly before going into core collapse unless they start far from the GC. In contrast, the boundary for $W_0 = 9$ lies at high initial mass and large number of particles, making the simulations of such clusters computationally impractical.

Another trend that can be seen in Table 1 is that more mass is accumulated at the center for clusters that start at larger distances from the GC. This is simply because there is more time available for the mass buildup. This does not necessarily mean that a heavier IMBH will be formed in these systems, as the fate of a very massive star being bombarded by other stars is not certain. Also, being the total available mass, this is strictly an *upper limit* to rather than an estimate of the IMBH mass.

In the rest of this section we present an analysis of the evolution of our Model 5c (see Figure 5), which started as a $W_0 = 9$ King model, with mass $m_0 = 2 \times 10^6 M_\odot$ at distance $R_0 = 10$ pc. This cluster went into core collapse very rapidly ($\gtrsim 10^5$ years) and reached the GC in about 5×10^5 years. After core collapse the central mass grew to a value $M_{\text{cen}} \simeq 5000 M_\odot$, which is consistent with the estimate, $M_{\text{cen}} \simeq 0.002 M_{\text{total}}$, by Gürkan et al.

(2004). The disruption of the cluster took place at $R_{\text{dis}} = 0.6$ pc from the GC.

4.2. Stars Stripped from the Cluster

During the inspiral, stars become unbound from the cluster as a result of the shrinking Jacobi radius. We present the mass distribution of these stars with respect to their distance from the GC in Figure 6, and the number of massive stars that leave the cluster within each distance bin in Figure 7. In these figures it is seen that the massive stars leave the cluster predominantly near disruption. This is because of mass segregation, but also because most stars leave the cluster near disruption and there are relatively few massive stars. As expected, the average mass of the stars that leave the cluster (indicated by the white line in Figure 6) slightly decreases throughout the inspiral (see also Fig. 7 of Gürkan et al. 2004). As the cluster evolves, massive stars sink towards the cluster center, leaving behind less massive stars which are preferentially removed. Our choice of initial conditions (requirement of core collapse before the end of inspiral) allows massive stars to segregate faster than the shrinking of the Jacobi radius because of the inspiral, so most of them remain bound throughout.

We present the surface density of initial masses of the stars that leave the cluster and compare this with the assumed mass density profile of the Galaxy in Figure 8. Throughout the inspiral, the contribution to the background surface density is small. The only detectable signature of a cluster inspiral will be the stars left behind that are significantly more massive and hence brighter than the stars of the Galactic background distribution.

4.3. The Cusp Retained at Disruption and IMBH

Near disruption, the cluster forms a power-law cusp, $\rho \propto r^{-\alpha}$, around the central point mass. We estimated the power-law exponent to be $1.35 < \alpha < 1.60$, which is compatible with the results of theoretical calculations (Bahcall & Wolf 1977) and N -body simulations (Preto et al. 2004; Baumgardt et al. 2004a,b) which yield a value $\simeq 1.55$.

The mass function of the stars in this cusp is quite different from the Salpeter IMF which we adopted at $t = 0$. The heavy part of the mass function is more populated because of mass segregation, even though the massive stars are preferentially removed via mergers with the central point mass. We show a comparison of the mass function for the innermost 2000 stars with the Salpeter IMF in Figure 9.

At disruption, the density of stars from the cluster exceeds the density of background stars. The (3-d) velocity dispersion at disruption is about 90 km s^{-1} . Since this is much

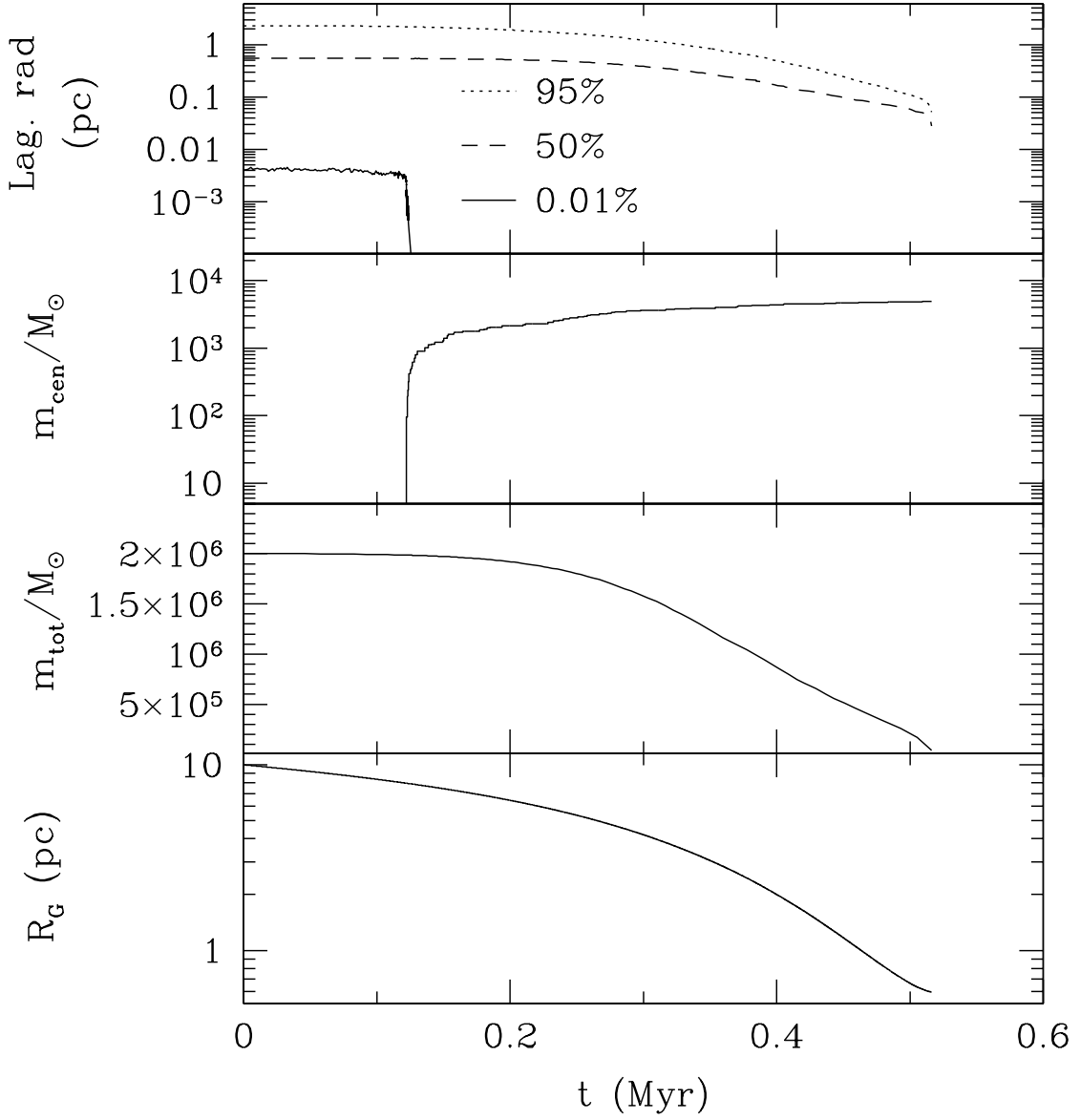


Fig. 5.— Evolution of Model 5c (see Table 1 for initial parameters). The top panel shows 0.01%, 50% and 95% Lagrange radii. The second panel is the growth of the central mass, starting at the core collapse. The third panel shows the evolution of the bound mass of the cluster and the bottom panel is the distance of the cluster from the GC.

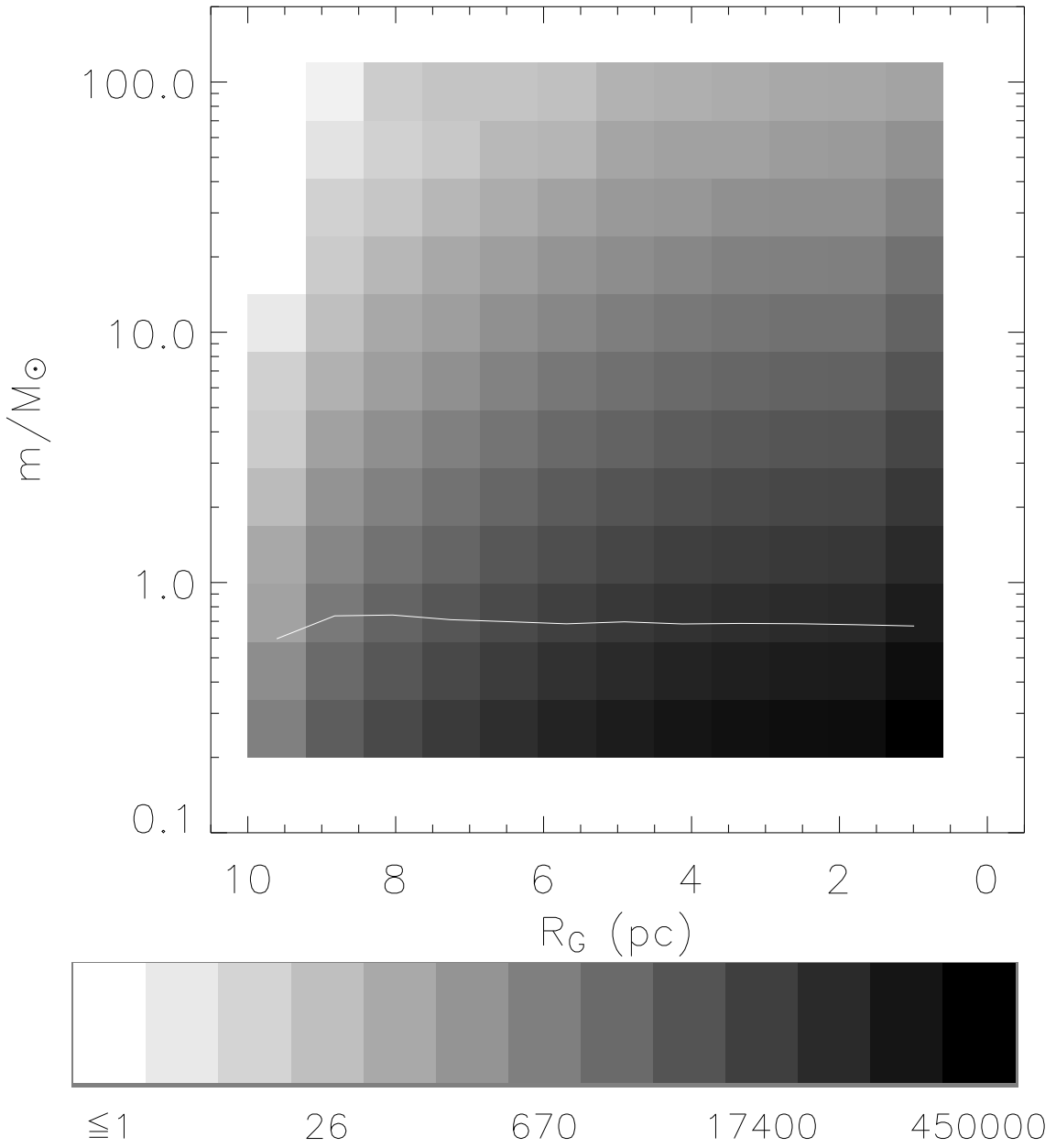


Fig. 6.— Mass and distance distribution of stars that leave the cluster during inspiral. The grey scale for the number of stars is logarithmic except for the ≤ 1 bin; the average mass in each distance bin is shown by a white line.

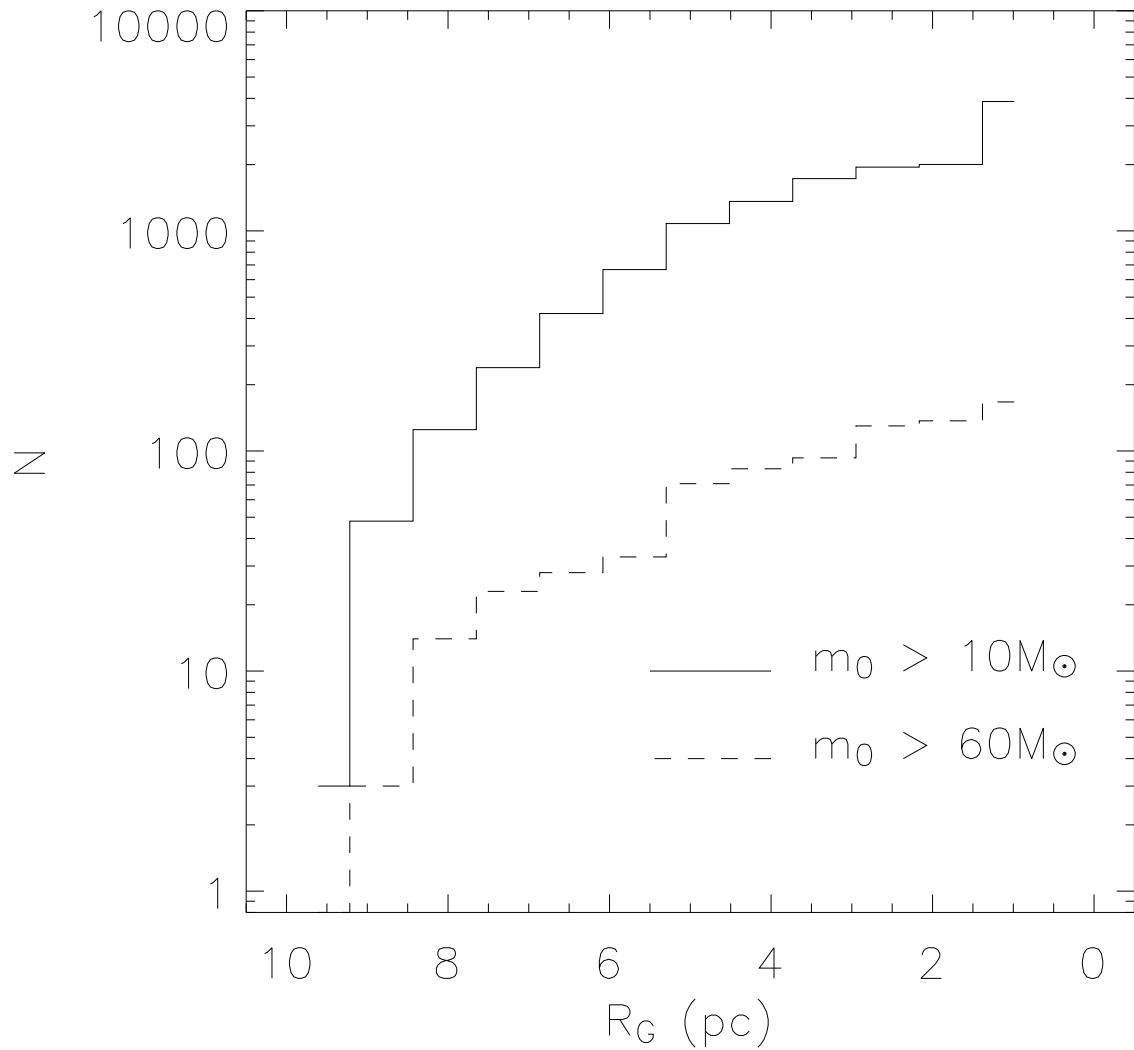


Fig. 7.— Number of massive stars that left the cluster at different distances from the GC. The solid and dashed lines indicate the stars whose initial mass is larger than $10M_\odot$ and $60M_\odot$, respectively.

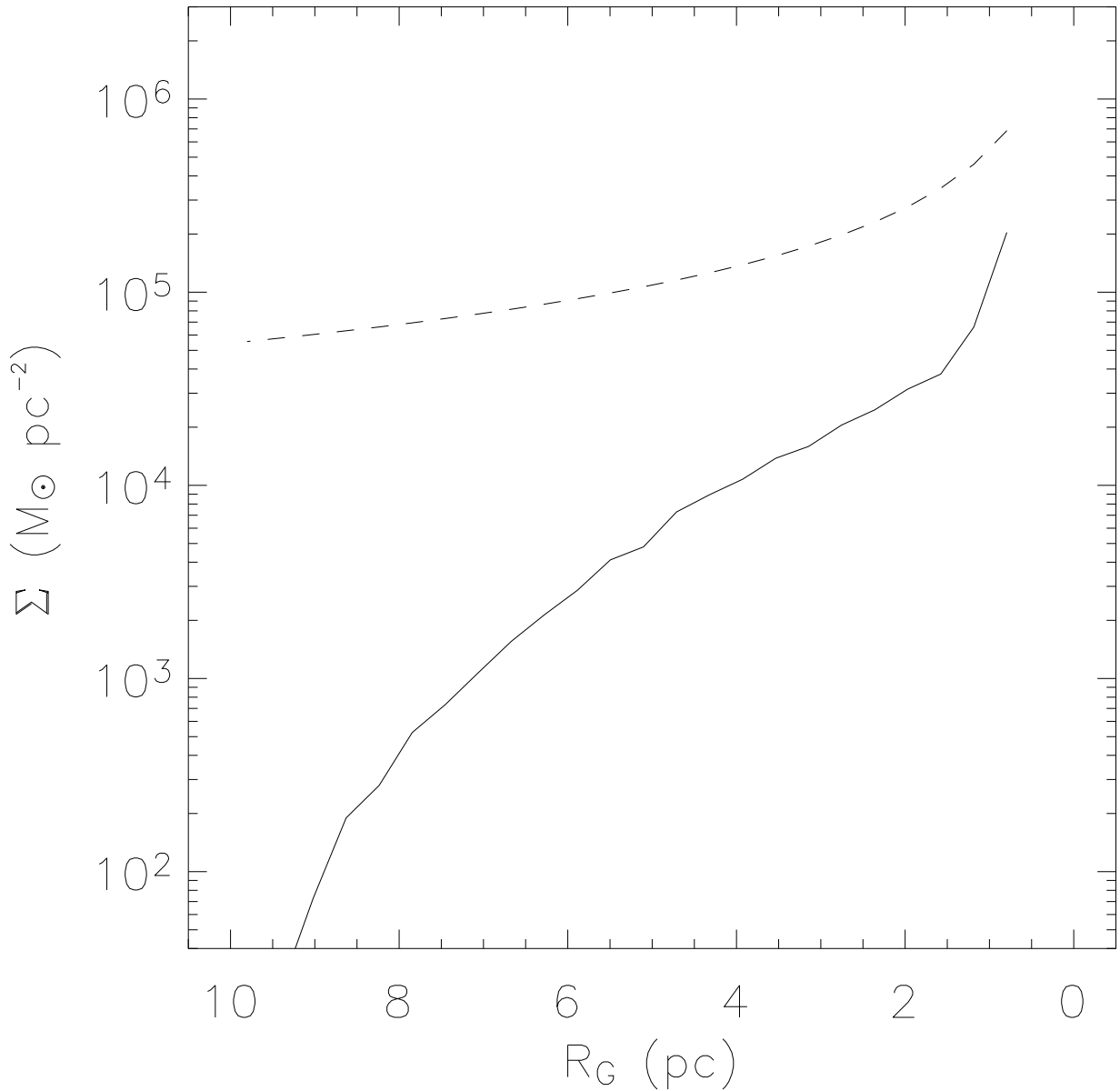


Fig. 8.— Surface density of stars that leave the cluster (solid line) compared with the Galactic mass density used in calculations (dashed line). Note that for the cluster, the surface density is calculated using the initial masses of the stars.

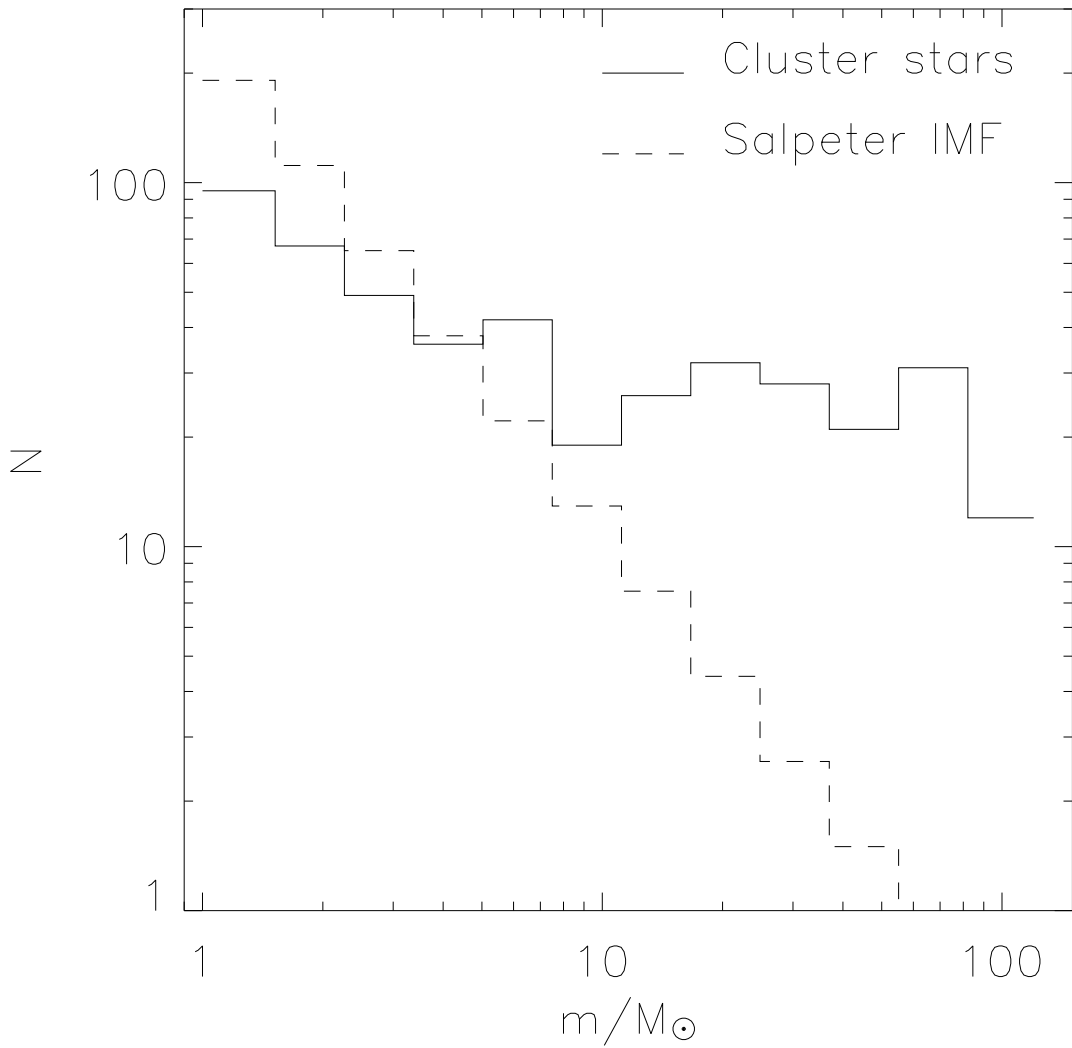


Fig. 9.— Comparison of the mass function for the innermost 2000 stars at cluster disruption (solid line) with the Salpeter IMF (dashed line; normalized to the same number of stars). The heavy part of the mass function at disruption is much more populated because of mass segregation.

smaller than the velocities near the GC, the stars would stay together and be observed as a clump, similar to the Central cluster (Figer 2004), or the rotating disk-like structures observed by Genzel et al. (2003) and Horrobin et al. (2004). Additionally, the stars which lie very close to the IMBH will remain bound to it longer than the stars lying outside, since these stars will be on Keplerian orbits and their relaxation time will be longer, preventing the expansion of the cluster. Such a collection of stars may exhibit a structure similar to that of the IRS 13E cluster observed by Maillard et al. (2004).

It is not possible to follow reliably the evolution of the cluster near disruption with our method, for several reasons. When the number of stars decreases to a very small value ($N \sim 1000$, see Hénon 1973, §2.4.1), the relaxation time becomes comparable to the dynamical time, making it necessary to take the effect of large-angle scatterings into account. This would be possible in principle, by incorporating these interactions into the Monte Carlo scheme in a way similar to collisions (Freitag & Benz 2002), if the rate of these events were low and the relaxation was still the dominant process for the evolution of the cluster. However, in this regime, the dynamical evolution, in particular the evaporation, of the cluster will not progress on a relaxation timescale and will depend sensitively on these large-angle scatterings. In addition, as the stars leave the cluster, the potential will get shallower. As a result, the restoring force on the central black hole, which keeps it near the cluster center, will decrease and its wandering will increase (which we do not model).

5. Discussion

The central parsec of our Galaxy hosts many young stars whose presence there poses a problem because of the unfavorable conditions for their formation. The range of age estimates and the peculiar dynamical properties (disk-like structures, clustering, possibility of larger than normal eccentricities) suggest that there is more than one mechanism at play. In this paper we consider one of the possibilities.

We investigated whether it is possible to explain the presence of the young massive stars near the GC by bringing them there as members of a cluster. At the same time, we want this cluster to form an IMBH, which can then make the stars in its vicinity migrate to inner orbits very near Sgr A*. This scenario requires: (1) rapid inspiral of the cluster, $t_{\text{in}} \lesssim 3 \text{ Myr}$; (2) the disruption to take place close to the GC, $R_{\text{dis}} \lesssim 1 \text{ pc}$; (3) the cluster to undergo core collapse during the inspiral to form an IMBH. Our work extends that of Gerhard (2001) and McMillan & Portegies Zwart (2003), who carried out semi-analytical calculations, and of Portegies Zwart et al. (2003), Kim & Morris (2003) and Kim et al. (2004), who used N -body simulations of dense clusters spiraling into the GC.

To determine the initial conditions suitable for this scenario, we carried out semi-analytical calculations and dynamical Monte Carlo simulations. A comparison of the results obtained by these methods showed that the change in the cluster structure has a considerable influence on the disruption distance. Following the evolution of the cluster also allowed us to draw conclusions about the demographics of the stars left behind and brought into the central parsec. The expansion of the outer parts of the cluster because of the relaxation enhances the mass loss and leads to earlier disruption.

Our simulations show that for clusters with $R_0 \gtrsim 10$ pc, an initial mass of at least $10^6 M_\odot$ is necessary. This is in agreement with the findings of Kim & Morris (2003). We also found that high concentrations ($W_0 \gtrsim 8$) are required to undergo core collapse during the inspiral. However, if the core collapse requirement is relaxed, clusters with moderate concentrations ($W_0 \sim 6$) can also survive the inspiral down to $R_{\text{dis}} < 1$ pc, starting with $R_0 \gtrsim 10$ pc and $m_0 \gtrsim 10^6 M_\odot$. This is because core collapse requires significant relaxation and clusters with low concentration cannot survive the accompanying expansion.

The density of the stars that leave the cluster during the inspiral is generally small compared to the Galactic background density, except near disruption. Almost all the massive stars that leave the cluster during the inspiral do so near disruption. As a result of the mass segregation, most of the cluster mass close to the IMBH is in heavy ($m > 10 M_\odot$) stars. Upon disruption, these stars will end up on orbits close to the IMBH. As a result of their proximity, they can then undergo strong interactions with the IMBH and possibly get scattered into orbits closer to the GC. If such clusters harboring IMBHs regularly form in the GC region, the central parsec may be hosting more than one IMBH and this process can be realized by participation of multiple IMBHs. The age spread of the young stars in the central parsec (~ 3 – 10 Myr) implies that there has been more than one instance of star formation in the recent history of the GC region.

Although the discussion in this paper has focused on our Galactic center, these ideas also have important consequences for other galaxies and for extragalactic astrophysics. The direct injection into the center of a galaxy of many IMBHs produced by collisional runaways in nearby young star clusters provides a potential new channel for building up the mass of a central SBH through massive BH mergers (Portegies Zwart & McMillan 2002). In contrast, minor mergers of galaxies are unlikely to produce massive BH mergers, as the smaller BH will rarely experience enough dynamical friction to spiral in all the way to the center of the more massive galaxy (Volonteri, Haardt, & Madau 2003). Our scenario has important consequences for LISA, the Laser-Interferometer Space Antenna, since the inspiral of an IMBH into a SBH provides an opportunity for direct study of strong field gravity and for testing general relativity (Collins & Hughes 2004; Culter & Thorne 2002; Phinney 2003).

Although the SBHs found in bright quasars and many nearby galactic nuclei are thought to have grown mainly by gas accretion (e.g. Fabian & Iwasawa 1999; Haehnelt, Natarajan, & Rees 1998; Richstone 2004; Soltan 1982), current models suggest that LISA will probe most efficiently a cosmological massive BH population of lower mass, which is largely undetected (Menou 2003). LISA will measure their masses with exquisite accuracy, and their mass spectrum will constrain formation scenarios for high-redshift, low-mass galaxies and, more generally, hierarchical models of galaxy formation (e.g. Haehnelt & Kauffmann 2002; Hughes & Holz 2003; Sesana, Haardt, Madau, & Volonteri 2004; Volonteri, Haardt, & Madau 2003).

The main difficulty with our scenario is the requirement of large initial cluster masses for rapid inspiral from $R_0 \gtrsim 10$ pc. A massive ($m_0 > 10^5 M_\odot$) cluster with a Salpeter IMF will contain a larger number of massive stars than currently observed at the GC region, both within and outside the central parsec. In particular, outside the central parsec, only a few young stars have been observed (Cotera et al. 1999), whereas we predict a larger number of these stars would have left the cluster during inspiral. There are multiple ways to resolve this problem, but it is not possible to determine by observation which, if any, of these mechanisms is most important. One of them is the formation of a cluster with a steeper IMF at the higher mass end, hence suppressing the number of massive stars. The upper mass cutoff we have chosen ($m_{\max} = 120 M_\odot$) is equivalent to introducing a steep IMF (Weidner & Kroupa 2004), but even more conservative choices are plausible (P. Kroupa, private communication). The requirement of a large initial mass is somewhat relaxed if the cluster is initially on an eccentric orbit (Kim et al. 2004). In this paper, we only considered circular orbits, so the mass requirements we find can be seen as upper limits. The problem of many young stars leaving the cluster during inspiral would be largely avoided by the presence of *initial* mass segregation, which is supported both by observations and theoretical arguments (Murray & Lin 1996; Bonnell & Davies 1998; Raboud & Mermilliod 1998; de Grijs et al. 2003). If the most massive members of the cluster start their life closer to the center, they will have less of a chance to leave the cluster outside the central parsec. We also note that the lack of observed young stars outside the central parsec could also result from higher extinction in this region (F. Yusef-Zadeh, private communication).

The initial mass function of the Arches cluster is thought to be significantly shallower than the Salpeter mass function (Figer et al. 1999; Kim et al. 2000). If a cluster is formed with a such an IMF, the central mass will grow faster and larger, since there are more massive stars. This may decrease the required total mass of the cluster, at the expense of increasing the fraction of mass in massive stars, since a larger central object can support a cluster more efficiently. We carried out a few simulations with shallower IMFs, power-law mass functions with $\alpha = 2.00$ and 1.75 . To make a fair comparison, we kept the total mass and the total number of stars in these cluster the same as in our Salpeter IMF models, and hence modified

the minimum mass in the cluster. This way, the relaxation time is kept constant, and the rate of expansion is expected to be similar for different IMFs. We found that, even though central masses up to twice as large were grown, the changes in the disruption distance were very small in these simulations. We conclude that growing a large enough central mass to have significant impact on this scenario (10% of initial total cluster mass Kim et al. 2004) is not possible by a modification of the IMF. Note that the mass function of the innermost 2000 stars at cluster disruption (Fig. 9), a result of the mass segregation, is very similar to what is observed in the Arches cluster (Stolte et al. 2002, Fig. 14). This indicates that the shallowness of the current mass function of the Arches can be explained by dynamical evolution, without the need for a shallow IMF.

The young compact cluster IRS 13E observed near the GC region provides strong support for the cluster inspiral scenario. This cluster has a projected diameter of $\sim 0.5''$ and is at a projected distance of $3.6''$ from Sgr A*. Its members have a common proper motion with velocity 280 km s^{-1} and no apparent common radial velocity, putting the cluster on an eccentric orbit. From these data Maillard et al. (2004) conclude that there is an IMBH at the center of this cluster with mass $\sim 750\text{--}1300 M_\odot$. It is possible that these stars are the central part of a larger cluster as in the five bright stars in the Quintuplet cluster, but N -body simulations show that such a cluster, consisting of about 2000 stars, will rapidly experience core collapse ($t_{\text{cc}} \sim 10^4 \text{ yr}$; H. Baumgardt, private communication). Even if there is no IMBH in the IRS 13E cluster, its presence is a strong indication that clustered star formation took place in the last few million years in the GC region, close enough to Sgr A* that part of the cluster is now within the central parsec of the Galaxy.

Alexander & Livio (2004) proposed that the young population observed very close ($< 0.05 \text{ pc}$) to Sgr A* are stars which reached this region on radial orbits and displaced stellar mass black holes that reside there. Gould & Quillen (2003) suggested that a member of this population, S0-2, is the remnant of a massive binary on an eccentric orbit which got disrupted by the supermassive black hole. These scenarios naturally complement the one we investigate in this paper. The stars scattered by the IMBH will end up on radial orbits and can further interact with and displace the stellar-mass black holes, or, if they are binaries, they can get disrupted while on these orbits. This will leave them on less eccentric orbits with smaller semimajor axes. The orbits of stars in the vicinity of an inspiraling IMBH have recently been investigated numerically by Levin et al. (2005), who showed that eccentric orbits with very small apocenter distances are possible if the inspiraling IMBH is on an eccentric orbit.

Despite these numerical investigations by Levin et al. (2005), the final fate of a cluster with an IMBH, which disrupts within the central parsec, remains highly uncertain. More

theoretical work is needed to understand both the final phases of the disruption and the interaction of the IMBH with the surrounding stars. Further observations of the GC, in particular proper motion measurements of the closest stars to understand their eccentricity distribution, and higher resolution observations of the IRS 13E cluster to resolve its structure and dynamics, will put constraints on the various scenarios proposed.

We thank Tal Alexander and Andrea Ghez for discussions about the mass distribution near the GC, Holger Baumgardt for providing his simulation results prior to publication, Marc Freitag, Miloš Milosavljević, Brad Hansen and Casey Law for useful discussions, Emrah Kalemci for help with the preparation of some of the figures, and Ruadhan O’Flanagan for comments on the manuscript. This work was supported by NASA Grants NAG5-13236, NNG04G176G and NSF Grant AST-0206276, and was finalized while MAG was at the Kavli Institute for Theoretical Physics at the University of California, Santa Barbara, as a Graduate Fellow.

A. Derivation of Inspiral Rate Formulae

In this appendix we derive the formulae for the inspiral rate dR/dt of a point mass, given a broken power-law Galactic mass distribution $M(R) \propto R^\alpha$, and an additional central point mass M_{SBH} . We use $R_b = 0.38 \text{ pc}$ to denote the breaking radius, and the subscripts 1 and 2 for regions $R \leq R_b$ and $R > R_b$ respectively. We follow and generalize the method of McMillan & Portegies Zwart (2003, see also Binney & Tremaine 1987 §7.1).

For $R \leq R_b$, the enclosed mass for a circular orbit is given by

$$M(R) = M_{\text{SBH}} + A_1 R^{\alpha_1}. \quad (\text{A1})$$

The potential corresponding to this mass distribution is

$$\phi(R) = -\frac{G M_{\text{SBH}}}{R} + \frac{G A_1 R^{\alpha_1-1}}{\alpha_1 - 1}, \quad (\text{A2})$$

and the circular velocity is given by

$$v_c(R)^2 = \frac{G M_{\text{SBH}}}{R} + G A_1 R^{\alpha_1-1}. \quad (\text{A3})$$

Combining these, we obtain the energy per unit mass for a circular orbit,

$$E_c(R) = -\frac{G M_{\text{SBH}}}{2R} + \frac{G A_1 R^{\alpha_1-1}}{2} \frac{\alpha_1 + 1}{\alpha_1 - 1}. \quad (\text{A4})$$

The acceleration resulting from the dynamical friction on an object of mass m is given by (Binney & Tremaine 1987, §7.1)

$$\mathbf{a}_f = -4\pi \ln \Lambda \chi G^2 \rho m \frac{\mathbf{v}_c}{v_c^3} \quad (\text{A5})$$

(see McMillan & Portegies Zwart 2003, for a description and numerical values of the constants). Hence the work done by dynamical friction per unit mass is

$$W_f = -4\pi \ln \Lambda \chi G^2 \frac{\rho m}{v_c}. \quad (\text{A6})$$

The time derivative of energy per unit mass in Equation (A4) is

$$\frac{dE_c}{dt} = \left(\frac{GM_{\text{SBH}}}{2R^2} + \frac{\alpha_1 + 1}{2} GA_1 R^{\alpha_1 - 2} \right) \frac{dR}{dt}. \quad (\text{A7})$$

By setting this equal to work done by dynamical friction, we obtain the following expression for orbital decay

$$\frac{dR}{dt} = \frac{-\chi \ln \Lambda G^{1/2} A_1 \alpha_1 m R^{(2\alpha_1 - 1)/2}}{(M_{\text{SBH}} + A_1 R^{\alpha_1} (\alpha_1 + 1)/2)(M_{\text{SBH}} + A_1 R^{\alpha_1})^{1/2}}, \quad (\text{A8})$$

or in dimensionless form

$$\frac{d\xi}{d\tau} = -\frac{2\pi \alpha_1 \chi \ln \Lambda m M_1}{(M_{\text{SBH}} + M_1)^{1/2}} \times \frac{\xi^{(2\alpha_1 - 1)/2}}{(M_{\text{SBH}} + M_1 \xi^{\alpha_1} (\alpha_1 + 1)/2)(M_{\text{SBH}} + M_1 \xi^{\alpha_1})^{1/2}}, \quad (\text{A9a})$$

where we have used

$$\xi \equiv \frac{R}{R_0}, \quad \tau \equiv \frac{t}{T_0}, \quad T_0 = 2\pi \left[\frac{R_0^3}{G(M_{\text{SBH}} + M_1)} \right]^{1/2}, \quad M_1 = A_1 R_0^{\alpha_1} \quad (\text{A9b})$$

with R_0 being the initial distance from the GC. For $R > R_b$ the equation for the enclosed mass takes the form

$$M(R) = M_{\text{SBH}} + A_1 R_b^{\alpha_1} - A_2 R_b^{\alpha_2} + A_2 R^{\alpha_2}. \quad (\text{A10})$$

Hence, the above formulae can be used for this regime by simply substituting 2 for 1 in subscripts and replacing M_{SBH} by $(M_{\text{SBH}} + A_1 R_b^{\alpha_1} - A_2 R_b^{\alpha_2})$. However, the above derivations are valid for $\alpha \neq 1$. For $\alpha_2 = 1$, which is the value indicated by observations (Genzel et al. 2003), a slightly different expression is obtained

$$\frac{d\xi}{d\tau} = -\frac{4\pi \chi \ln \Lambda M_2 m}{(M_{\text{SBH}} + A_1 R_b^{\alpha_1} - A_2 R_b + M_2)^{1/2}} \times \frac{\xi^{1/2}}{(M_{\text{SBH}} + A_1 R_b^{\alpha_1} - A_2 R_b + M_2 \xi)^{3/2}}, \quad (\text{A11a})$$

where

$$\xi \equiv \frac{R}{R_0}, \quad \tau \equiv \frac{t}{T_0}, \quad T_0 = 2\pi \left[\frac{R_0^3}{G(M_{\text{SBH}} + A_1 R_b^{\alpha_1} - A_2 R_b + M_2)} \right]^{1/2}, \quad M_2 = A_2 R_0. \quad (\text{A11b})$$

For R given in pc, $A_1 = 2.46 \times 10^6 M_{\odot}$, and $A_2 = 2.18 \times 10^6 M_{\odot}$ according to values quoted by Genzel et al. (2003).

REFERENCES

Alexander, T., & Livio, M. 2004, ApJ, 606, L21

Alexander, T., & Morris, M. 2003, ApJ, 590, L25

Bahcall, J. N., & Wolf, R. A. 1977, ApJ, 216, 883

Baumgardt, H., Makino, J., & Ebisuzaki, T. 2004a, ApJ, 613, 1133

—. 2004b, ApJ, 613, 1143

Binney, J., & Tremaine, S. 1987, Galactic dynamics (Princeton, NJ, Princeton University Press)

Bonnell, I. A., & Davies, M. B. 1998, MNRAS, 295, 691

Collins, N. A. & Hughes, S. A. 2004, Phys. Rev. D, 69, 124022

Cotera, A. S., Simpson, J. P., Erickson, E. F., Colgan, S. W. J., Burton, M. G., & Allen, D. A. 1999, ApJ, 510, 747

Culter, C., & Thorne, K. 2002, in proceedings of the 16th International Conference on General Relativity and Gravitation, ed. N.T. Bishop & D. Maharaj Sunil. (World Scientific, Singapore), 72

Fabian, A. C. & Iwasawa, K. 1999, MNRAS, 303, L34

Figer, D. F. 2004, in ASP Conf. Ser. 322, The formation and evolution of massive young star clusters, eds. H.J.G.L.M. Lamers, L.J. Smith & A. Nota, 49, [astro-ph/0403088](#)

Figer, D. F., Kim, S. S., Morris, M., Serabyn, E., Rich, R. M., & McLean, I. S. 1999, ApJ, 525, 750

Fregeau, J. M., Cheung, P., Portegies Zwart, S. F., & Rasio, F. A. 2004, MNRAS, 352, 1

Fregeau, J. M., Gürkan, M. A., Joshi, K. J., & Rasio, F. A. 2003, ApJ, 593, 772

Freitag, M., & Benz, W. 2002, A&A, 394, 345

Freitag, M., Gürkan, M. A., & Rasio, F. A. 2004, in Proceedings of "Massive Stars in Interacting Binaries" (Lac Sacacomie, Quebec, 16-20 Aug 2004), [astro-ph/0410327](#)

Freitag, M., Gürkan, M. A., & Rasio, F. A. 2005b, submitted to MNRAS, [astro-ph/0503130](#)

Freitag, M., Rasio, F. A., & Baumgardt, H. 2005, submitted to MNRAS, [astro-ph/0503129](#)

Genzel, R., Schödel, R., Ott, T., Eisenhauer, F., Hofmann, R., Lehnert, M., Eckart, A., Alexander, T., Sternberg, A., Lenzen, R., Clénet, Y., Lacombe, F., Rouan, D., Renzini, A., & Tacconi-Garman, L. E. 2003, *ApJ*, 594, 812

Gerhard, O. 2001, *ApJ*, 546, L39

Ghez, A. M., Duchêne, G., Matthews, K., Hornstein, S. D., Tanner, A., Larkin, J., Morris, M., Becklin, E. E., Salim, S., Kremenek, T., Thompson, D., Soifer, B. T., Neugebauer, G., & McLean, I. 2003, *ApJ*, 586, L127

Ghez, A. M., Salim, S., Hornstein, S. D., Tanner, A., Lu, J. R., Morris, M., Becklin, E. E., & Duchêne, G. 2004, *ApJ*, in press, [astro-ph/0306130](#)

Giersz, M. 2001, *MNRAS*, 324, 218

Gould, A., & Quillen, A. C. 2003, *ApJ*, 592, 935

de Grijs, R., Gilmore, G. F., & Johnson, R. A. 2003, in The Local Group as an Astrophysical Laboratory, STScI Symp., May 2003, Baltimore (USA), ed. Livio M, [astro-ph/0305262](#)

Gürkan, M. A., Freitag, M., & Rasio, F. A. 2004, *ApJ*, 604, 632

Gürkan, M. A., & Rasio, F. A. 2004, in IAU Symposium 222: “The interplay among Black Holes, Stars and ISM in Galactic Nuclei”, Thaisa Storchi Bergmann, Luis C. Ho and Henrique R. Schmitt, eds., Cambridge University Press., in press

Haehnelt, M.G., & Kauffmann, G. 2002, *MNRAS*, 336, L61

Haehnelt, M. G., Natarajan, P., & Rees, M. J. 1998, *MNRAS*, 300, 817

Hansen, B. M. S., & Milosavljević, M. 2003, *ApJ*, 593, L77

Hénon, M. 1971, *Ap&SS*, 14, 151

Hénon, M. 1973, in Saas-Fee Advanced Course 3: Dynamical Structure and Evolution of Stellar Systems, 183

Hénon, M. 1975, in IAU Symp. 69: Dynamics of the Solar Systems, 133

Horrobin, M., Eisenhauer, F., Tecza, M., Thatte, N., Genzel, R., Abuter, R., Iserlohe, C., Schreiber, J., Schegerer, A., Lutz, D., Ott, T., & Schödel, R. 2004, *Astronomische Nachrichten*, 325, 88

Hughes, S.A., & Holz, D.E. 2003, *Class. Quant. Grav.*, 20, 65

Joshi, K. J., Nave, C. P., & Rasio, F. A. 2001, *ApJ*, 550, 691

Joshi, K. J., Rasio, F. A., & Portegies Zwart, S. 2000, *ApJ*, 540, 969

Kim, S. S., Figer, D. F., & Morris, M. 2004, *ApJ*, 607, L123

Kim, S. S., & Morris, M. 2003, *ApJ*, 597, 312

Kim, S. S., Figer, D. F., Lee, H. M., & Morris, M. 2000, *ApJ*, 545, 301

Levin, Y., Wu, A. S. P., & Thommes, E. W. 2005, [astro-ph/0502143](#)

Maillard, J. P., Paumard, T., Stolovy, S. R., & Rigaut, F. 2004, *A&A*, 423, 155

McMillan, S. L. W., & Portegies Zwart, S. F. 2003, *ApJ*, 596, 314

Melia, F., & Falcke, H. 2001, *ARA&A*, 39, 309

Menou, K. 2003, *Class. Quant. Grav.*, 20, S37

Murray, S. D., & Lin, D. N. C. 1996, *ApJ*, 467, 728

Phinney, E.S. 2003, Science with LISA: high precision for black holes, cosmology and white dwarf binaries, American Astronomical Society, HEAD Meeting 35, #27.03

Portegies Zwart, S. F., Baumgardt, H., Hut, P., Makino, J., & McMillan, S. L. W. 2004, *Nature*, 428, 724, [astro-ph/0402622](#)

Portegies Zwart, S. F., & McMillan, S. L. W. 2002, *ApJ*, 576, 899

Portegies Zwart, S. F., McMillan, S. L. W., & Gerhard, O. 2003, *ApJ*, 593, 352

Preto, M., Merritt, D., & Spurzem, R. 2004, *ApJ*, 613, L109

Raboud, D., & Mermilliod, J.-C. 1998, *A&A*, 333, 897

Richstone, D. 2004, in *Coevolution of Black Holes and Galaxies*, ed. L.C. Ho (Cambridge Univ. Press, Carnegie Obs. Ast. Ser. Vol. 1), 281

Quinn, T., Tremaine, S., & Duncan, M. 1990, *ApJ*, 355, 667

Schödel, R., Ott, T., Genzel, R., Eckart, A., Mouawad, N., & Alexander, T. 2003, *ApJ*, 596, 1015

Sesana, A., Haardt, F., Madau, P., & Volonteri, M. 2004, *ApJ*, 611, 623

Soltan, A. 1982, *MNRAS*, 200, 115

Stolte, A., Grebel, E. K., Brandner, W., & Figer, D. F. 2002, *A&A*, 394, 459

Volonteri, M., Haardt, F., & Madau, P. 2003, *ApJ*, 582, 559

Weidner, C., & Kroupa, P. 2004, *MNRAS*, 348, 187